

THIRD EUROPEAN ROTORCRAFT AND POWERED LIFT AIRCRAFT FORUM

Paper No. 54

THEORETICAL MODELING OF HIGH SPEED
HELICOPTER IMPULSIVE NOISE

FREDRIC H. SCHMITZ

YUNG H. YU

Ames Directorate, Air Mobility R&D Laboratory
U.S. Army Aviation R&D Command
Moffett Field, California, U.S.A.

September 7-9, 1977

AIX-EN-PROVENCE, FRANCE

ASSOCIATION AERONAUTIQUE ET ASTRONAUTIQUE DE FRANCE

THEORETICAL MODELING OF HIGH SPEED

HELICOPTER IMPULSIVE NOISE

Fredric H. Schmitz
Yung H. Yu

Ames Directorate, Air Mobility R&D Laboratory
U.S. Army Aviation R&D Command
Moffett Field, California, U.S.A.

SUMMARY

A simple theoretical model of high speed helicopter impulsive noise is developed which depends primarily on the large scale features of the rotor's aerodynamic flow field. For acoustic radiation near the rotor's tip-path-plane, monopole, dipole, and quadrupole sources all contribute — with the latter term dominating for helicopter advancing tip Mach numbers (M_{AT}) greater than 0.5. Predicted peak amplitudes and temporal shape show good correlation with experiment for the UH-1H helicopter operating below $M_{AT} = 0.9$. Above $M_{AT} = 0.9$, theoretical-experimental comparison is less favorable. It is postulated that the differences at high advancing tip Mach numbers are traceable to unsteady transonic aerodynamic and acoustic effects.

1. Introduction

Helicopter impulsive noise, sometimes called "blade slap," is one of the most annoying and easily detectable sounds generated by a helicopter; it is also one of the more challenging topics of helicopter research. Many theoretical approaches have been developed over the years to explain the aerodynamic and acoustic causes of impulsive noise, but they have been only partially successful. However, in recent years the situation has been changing rapidly. New quantitative experimental results are available to check theoretical analyses and to help guide the theoretical researcher — helping him to develop mathematical models that accurately describe the physical phenomena of impulsive noise.

A typical half period of a two-bladed rotor that is generating impulsive noise is shown in Fig. 1 (from Ref. 1). The data were acquired using an in-flight measurement technique with the microphone located directly in front of the helicopter and essentially in plane with the rotor tip-path-plane. Two distinct sources of noise are present: a combination of positive and negative pressure spikes which are known to be dependent upon blade-vortex interactions, followed by a large negative pressure pulse whose shape and amplitude are extremely sensitive to advancing tip Mach numbers. This latter pulse, called high-speed impulsive noise, is the topic of this paper. This periodic phenomenon is known to occur on most helicopters in high-speed forward flight, radiating large amounts of acoustic energy in front of the helicopter near the rotor tip-path-plane.

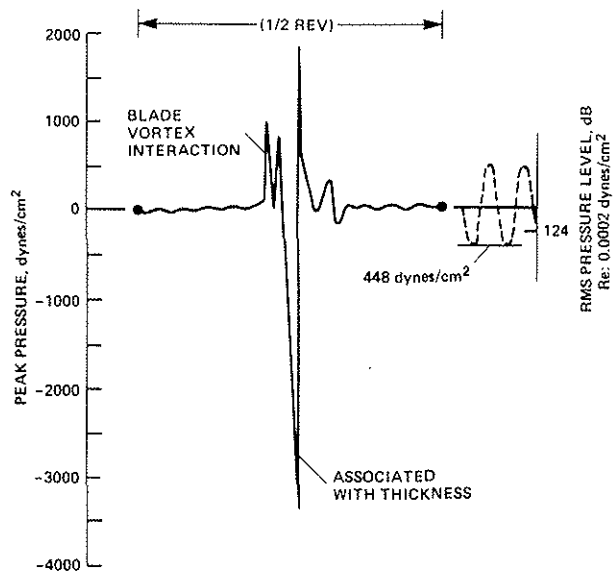


Fig. 1. Composite illustration showing dominant UH-1H acoustic waveform features (from Ref. 1).

The first simple theoretical model of rotor noise was developed by Gutin² who recognized that steady aerodynamic forces on a propeller act as acoustic dipole sources. Working in the frequency domain, he was able to show that the first few harmonics of rotor noise were related to the steady thrust and drag forces on the propeller. In his simple theory, net forces were assumed to be acoustic dipoles acting at a distinct point along the blade. Thus, he neglected the distributed nature of the forces and the retarded time effect — a "compact" source assumption. Garrick and Watkins³ extended this work to the case of the uniformly moving propeller. At about the same time, Deming⁴ looked into the effect of blade thickness on the radiated noise. He replaced a symmetric airfoil by an infinite number of line pistons (sources and sinks) to match the boundary condition of no flow through the rotor airfoil surface. Deming assumed, as Gutin had, that the problem was compact, that is, that there were no retarded time differences between the sources and sinks at any given radial station along the airfoil. Deming's comparison with experiment was less impressive than that of Gutin's — the major finding was that thickness noise was not a major contributor to the periodic noise of propellers. At the time the research efforts were beginning to focus on discrepancies between experimental results at high tip speeds and available theories, emphasis on jet propulsion became popular, and most comprehensive efforts were halted.

Fundamental noise research was, however, increasing in level and scope. Lighthill⁵ formulated an exact acoustic analogy for sound due to turbulence. Curle⁶ extended this formulation to include the effects of solid surfaces. Meanwhile, operational experience identified the acoustic detection problem as important to combat survivability of the military helicopter. This initiated much research into potential causes of helicopter periodic noise — the two most notable efforts were made by Lawson⁷ and Wright.⁸ Taking Lighthill's stationary model, Lawson and Wright argued that in addition to steady forces (identified by propeller researchers as causes of periodic noise) the unsteady forces that the rotor blade experiences as it traverses one revolution are very efficient radiators of periodic noise. They suggested that in order to predict the higher harmonics of radiated noise, one could use a compact source model but would need to know very high harmonics of blade loading. Although the agreement with experiment was not consistent, their theories did show more encouraging correlation with the limited experimental frequency domain data available.

In this same time period, Lyon⁹ looked at monopole thickness and dipole force noise of the helicopter rotor by replacing the blade by a progression of accelerating "torpedoes." Using this unconventional approach, he found that monopole thickness effects may be important at advancing tip Mach numbers near unity. At about the same time, Arndt and Borgman¹⁰ applied the fluctuating loads theory to the helicopter rotor under similar conditions and related the high speed impulsive noise to the drag divergence phenomenon at high advancing tip Mach numbers. Although this latter approach was used in many helicopter preliminary designs, it was never quantitatively checked with experiment. The lack of high quality time domain impulsive noise data made it impossible to trace cause and effect mechanisms to validate either theory. At about this same time Ffowcs Williams and Hawkings¹¹ rederived the classical acoustic equations for bodies moving at high Mach numbers with respect to the medium. Their contributions emphasized the noncompactness of the problem and set up the basic theoretical formulation in use today.

More recently, Farassat¹² and Hawkings and Lawson¹³ applied the Ffowcs Williams and Hawkings formulation to the high tip speed rotor problem. Using noncompact monopole terms to represent thickness and distributed dipoles to represent localized pressure, Farassat has reported close agreement in peak amplitude and shape with test data. His method of solving the basic equations was a straightforward numerical evaluation of the integral solution in the time domain. Lawson,¹⁴ using similar assumptions but working in the frequency domain and comparing results with the data of Ref. 1, reported agreement with experimental data within 3-6 dB for a number of measurement points. The present

authors have also applied similar techniques utilizing monopoles to represent thickness and dipoles to represent local forces and have obtained results similar to those of Lowson. In almost every case, the peak pressure amplitude at a point located in the path of maximum radiated high speed impulsive noise, was underpredicted by a factor of approximately 2. In addition, the calculated pressure-time history matched the experimental pulse shape only at the lower advancing tip Mach numbers.

Although it is tempting to blame the generally poor correlation of theory and experiment on experimental error, the data used to check the theory have been gathered on a number of experimental programs. The experimental data are not only consistent, but scale remarkably well in shape and amplitude for both model and full scale tests.¹⁵ Thus, one is drawn to the inevitable conclusion that the theoretical modeling is not yet adequate. One would suspect that some important physical considerations have been omitted in the construction of the basic mathematical model — a hypothesis this paper will attempt to prove.

Although the general integral solution to the wave equation for sources in motion¹¹ is straightforward, a physical interpretation of the acoustic sources is more subtle. The main difficulties arise because the geometry of the rotating helicopter blade is so complex, when viewed in a nonrotating reference frame, that simple analytical solutions are not readily available. Those that have been attempted (e.g., Ref. 13) usually rely on a frequency domain approach. This is quite unnatural because of the impulsive nature of the event which results in many harmonics of noise. The direct approach is also not without problems. Near $M = 1.0$, mathematical singularities arise¹² which should be considered in the numerical computation of the time domain pressure. This can lead to rather large, complex computer programs in which it may be difficult to determine the significance of key design parameters. However, working in the time domain is a more logical approach and by careful choice of analytical techniques for the problem at hand, most of these removable singularities can be handled quite well.

It will be shown in this paper that very simple models can yield good correlation with experimental data for the advancing tip Mach numbers that are important in current helicopter operations. In this theoretical model, the number of singularities are kept to the minimum necessary to describe the physical event; but in addition to monopoles and dipoles, quadrupole sources are shown to be involved in the basic formulation of the problem. The idea that quadrupoles might be radiators of acoustic energy is really not new — it has been suggested by many researchers. In fact, Ffowcs Williams and Hawkins,¹⁶ arguing from order of magnitude considerations, suggested that quadrupoles could be the most efficient generators of discrete fan tone noise. The development of the present simple acoustic model allows a direct numerical evaluation of this important phenomenon, and quantitatively shows that quadrupole thickness effects need to be considered in the modeling of high-speed helicopter impulsive noise.

2. Basic Theoretical Approach

The general acoustic problem for sound generated by moving surfaces was investigated extensively using general function theory.¹¹ The formal solution, given in Eq. 1, implies that the acoustic field generated by moving surfaces is determined by not only the boundary conditions on the surface^{12,13} but also by the local disturbed flow field off the surface.

$$4\pi a_0^2 \rho'(\vec{x}, t) = \frac{\partial}{\partial t} \int \left[\frac{\rho_0 u_n}{r|1-M_r|} \right]_{\text{ret}} dS(\vec{y}) - \frac{\partial}{\partial x_i} \int \left[\frac{p_{ij} n_j}{r|1-M_r|} \right]_{\text{ret}} dS(\vec{y}) + \frac{\partial^2}{\partial x_i \partial x_j} \int \left[\frac{T_{ij}}{r|1-M_r|} \right]_{\text{ret}} dV(\vec{y}) \quad (1)$$

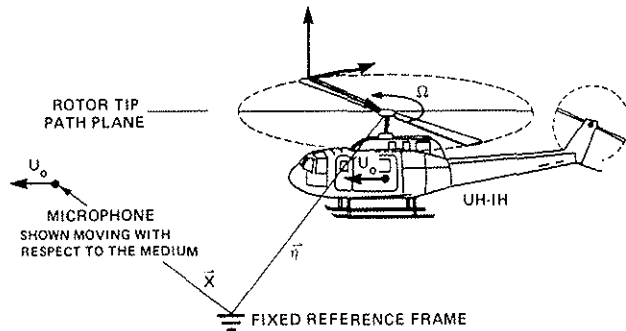
where $T_{ij} = \rho u_i u_j + p_{ij} - a_0^2 \rho \delta_{ij}$ and standard notations are used.

The right-hand side of Eq. (1) contains three types of "acoustic sources." The first is a monopole source which is governed by the local time rate of change of mass displaced by the moving surface. The second term is a dipole source which is dependent upon a spatial derivative of local surface forces. The third and last term is a quadrupole source — a source which is often omitted in many descriptions of noise from moving surfaces. Its shape and magnitude are governed by two spatial derivatives of the T_{ij} stress tensor in the volume of fluid surrounding the moving surface.

In principle, Eq. (1) is the solution to the high-speed rotor problem, because the rotor problem is really just a specialized case of the more general acoustic problem of surfaces in motion. However, interpreting the acoustic geometric complexities of the rotating blade and then choosing correct aerodynamic boundary conditions for each acoustic source on the right-hand side of Eq. (1) are not trivial problems. Both aspects of this solution procedure are treated in the following discussions.

3. Some Acoustic Geometry

A three-dimensional sketch of the geometries involved in the helicopter acoustic problem is given in Fig. 2. The rotor, located at position \vec{r} , is



rotating about the hub at an angular rate Ω and translating through air at a constant velocity \vec{U}_0 . The observer (or microphone) is located at position \vec{x} and can be considered stationary or to be moving at the translational speed of the helicopter, U_0 , through the medium. Stationary ground-mounted microphones are customary for "fly-by" testing and the moving microphone is necessary when acoustic data is gathered in-flight¹ or in wind tunnels.¹⁵

Fig. 2. Basic acoustic geometry.

There are several procedural methods of evaluating Eq. (1) (Refs. 12 and 13) for translating rotors. Although the methods have weaknesses, each has strong points that can be used to advantage for certain classes of problems. For the more common rotorcraft problems, the advancing tip Mach numbers never exceed 1 and, thus, the integrable singularities appearing in each right-hand side term cause no real numerical evaluation problem. Therefore, a straightforward numerical solution is simple and physically enlightening. The apparent complexities are due to geometry and the correct treatment of retarded time.

One of the first tasks in the construction of a solution is the development of a form that is easily calculable and physically interpretive. The mix of spatial and time differentiation in Eq. (1) is numerically cumbersome. However, in the acoustic far field, Eq. (1) can be rewritten as

$$4\pi a_0^2 \rho'(\vec{x}, t) \approx \frac{\partial}{\partial t} \int \left[\frac{\rho_0 u_n}{r|1 - M_r|} \right]_{\text{ret}} dS(\vec{y}) + \frac{1}{a_0} \frac{\partial}{\partial t} \int \left[\frac{p_1 \cos \theta_1}{r|1 - M_r|} \right]_{\text{ret}} dS(\vec{y}) + \frac{1}{a_0^2} \frac{\partial}{\partial t} \int \left[\frac{\cos \theta_1 \cos \theta_2}{r|1 - M_r|} \frac{\partial T_{ij}}{\partial t} \right]_{\text{ret}} dV(\vec{y}) \quad (2)$$

where $\cos \theta_1, \cos \theta_2$ denote directional cosines between axis of acoustic

sources and \vec{r} . In this expression (Eq. (2)), only time differentiation of all three acoustic sources is necessary.

For simplicity of interpretation, the following arguments consider the in-plane radiation of impulsive noise only.* An aerial view of the in-plane radiation problem for a microphone moving at the same speed as the helicopter is shown in Fig. 3. A simple point source of sound is assumed to be emitted at position P and to arrive at the position of the moving observer, O', at some later time, r/a_0 . The velocity of the point P at any instant of time is $\vec{U}_0 + \vec{\Omega}R$, and M_r is the component of that velocity vector along the r direction divided by the speed of sound.

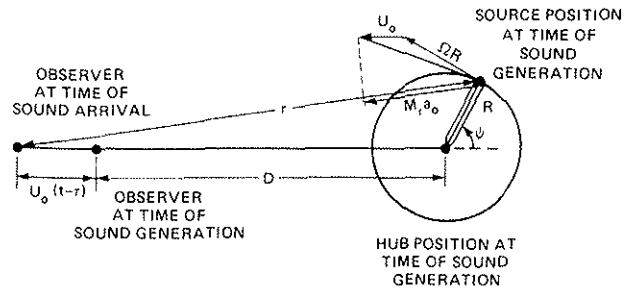


Fig. 3. Top view of rotor acoustic in-plane geometry.

As in all acoustic problems, correct treatment of the retarded time operator is essential. From the given geometry, observer time t is related to emission time τ by the implicit relationship

$$\tau = t - \frac{r(t, \tau)}{a_0} \quad (3)$$

where

$$r^2 = \left(D + R \cos \psi + U_0 \frac{r}{a_0} \right)^2 + (R \sin \psi)^2 \quad (4)$$

and the term $(U_0/a_0)r$ is necessary to represent the effect of observer motion. Therefore, a point source which was emitted at the retarded time τ takes time $r(t, \tau)/a_0$ to travel the distance r arriving at time t . If the rotor is rotating at angular velocity Ω , then pulses that are emitted at selected azimuthal positions, ψ ($\psi = \Omega\tau$) obey the expression

$$\Omega\tau = \psi = \Omega t + \frac{\Omega r(t, \tau)}{a_0} \quad (5)$$

which is plotted in Fig. 4a. This figure shows that, as the Mach number approaches 1, a large region of blade azimuth contributes to a narrow pulse width. The result is an inherent amplification of local source effects by the factor $(d\tau/dt)$ which is illustrated in Fig. 4b.

Part of this amplification of acoustic energy is explicitly accounted for in Eq. (2). The doppler factor $1/(1-M_r)$, which is the Jacobian of a coordinate transformation, already appears in each acoustic source term and represents the formation of a velocity potential wave with respect to the medium. A second doppler factor is implicit in Eq. (2) and does not enter until the time derivative of the potential function is taken. This doppler factor can incorporate uniform observer motion. In each case large amplification effects are evident as advancing Mach numbers approach 1. These simple expressions show that the blade tip is acoustically the most efficient portion of the rotor, with acoustic efficiency decaying rapidly for inboard radial positions. It can also be concluded from Fig. 4b that the dominant azimuthal source position is near the tangency point of a straight line drawn from the observer to the circle

*This is not a real limitation to what is being presented, because impulsive noise is known to be at a maximum within the tip path plane of the rotor.¹ Furthermore, the fundamental procedure is applicable to out-of-plane acoustic radiation and is used in a later section to calculate longitudinal directivity profiles of radiated noise.

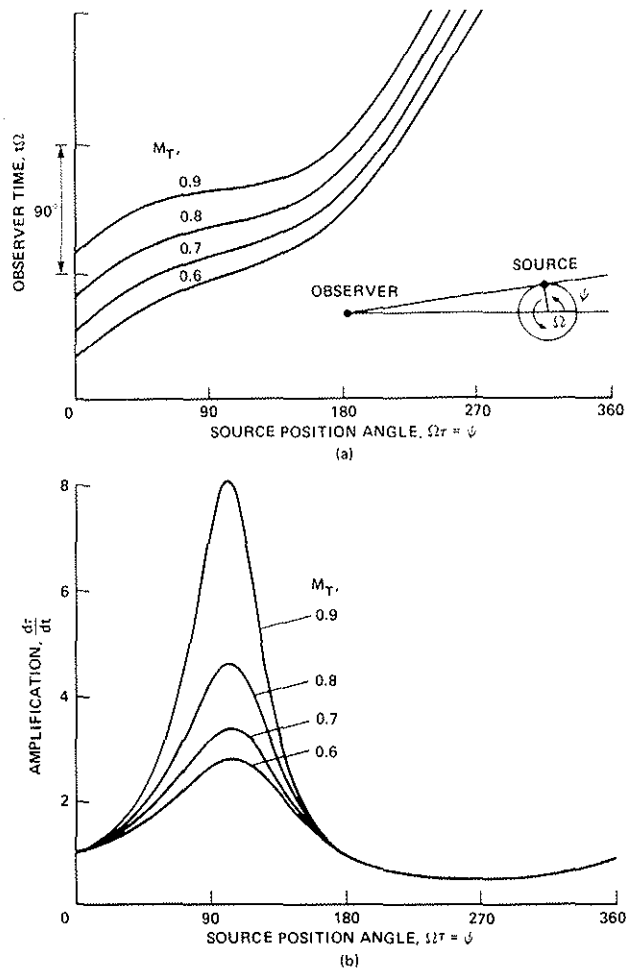


Fig. 4. Retarded time factors.

The details of this solution procedure are outlined in the appendix. Its simplicity, both numerically and conceptually, adds insight to the entire noise generation process. The most complex calculation presented in this paper requires no more than 5 sec of CDC 7600 execution time.

4. Acoustic Sources

The second half of the numerical evaluation of Eq. (2) involves the mathematical description of the three source terms. Once their strength and physical origins have been modeled, each term is then used as input to the solution procedure outlined in the preceding section. The result is the far field pressure time history of the radiated noise for each grouping of acoustic sources.

Monopole

The first and most obvious source of radiated far field noise is mathematically represented by the monopole term

$$\frac{\partial}{\partial t} \int \left[\frac{\rho_0 u_n}{r|1 - M_r|} \right] dS(\vec{y})$$

Physically, the term represents the equivalent acoustic source that is created because each segment of the finite thick rotor blade must displace mass as it moves through the medium. Thus, the portions of the blade that push fluid away from the blade are represented as acoustic monopole sources while those that

described by the tip of the rotor (Fig. 4b). At this azimuthal position, all line sources along the rotor blade arrive at the observer position at approximately the same time.

These physical insights are quite useful in the construction of a numerical scheme to evaluate Eq. (2). It is straightforward to choose blade coordinates in the numerical discretization of each of the two blade surface integrals and the exterior volume integral. Simple spacing of elemental areas and volumes according to blade geometry is quite natural. However, all signals that arrive at an observer position at time t , were emitted at some earlier time τ . Thus, it is expedient to iterate on the retarded time equation to find each elemental source's position in ψ space and then calculate its contribution to the acoustic field at time t . By adopting this simple iteration procedure (outlined in the appendix), no numerical interpolation is required. By choosing observer time increments according to given positions of ψ (see Eq. (5)), an adequate number of points is ensured where the function is amplified the most. When the final time differentiation is applied, a smooth differentiable function results.

close the body (or reattach the flow) act as sinks. A sketch of the resulting flow over a two-dimensional airfoil section is given in Fig. 5a. From small-perturbation theory for a slender two-dimensional body, the normal component of surface velocity is expressed as follows:

$$u_n \approx U_o \cdot (\text{local surface slope}) \quad (6)$$

where U_o is the local freestream velocity of the blade element.

The integral of the monopole sources can be evaluated by dividing the blade into chordwise and spanwise elements and summing each contribution according to the geometric rules developed in the preceding section. Thus, the monopole source becomes

$$2 \frac{\partial}{\partial t} \sum_{k=1}^{\ell} \sum_{i=1}^n \rho_o \left[\frac{U_o \left(\frac{dy_2}{dy_1} \right)_{ki}}{r |1 - M_r|} \right] dy_{1_i} dy_{3_k} \quad (7)$$

Although it is tempting to immediately divide (discretize) the blade into many chordwise and spanwise stations, a more physically rewarding procedure is to take as few stations as possible to describe the flow. Remembering that the blade tip is the most efficient radiator of noise, the first model considered represents only the outer 10% of the rotor blade. The effective chordwise line of two-dimensional monopole sources is then assumed to act at the 95% radial location. The numerical representation becomes

$$2 \frac{\partial}{\partial t} \sum_{i=1}^n \rho_o \left[\frac{U_o \left(\frac{dy_2}{dy_1} \right)_i}{r |1 - M_r|} \right] (0.1 R) (dy_{1_i}) \quad (8)$$

Similarly, the chordwise distribution of sources can be approximated in the simplest case by two monopole singularities: a source of strength $2U_o \Delta y_{\max}$ and a sink of strength $-2U_o \Delta y_{\max}$, where Δy_{\max} is half of the maximum thickness of a blade. A sketch of the approximate location of these singularities is given in Fig. 5b. Notice that near the rotor blade the local aerodynamic flow is badly distorted by considering this simplest of source models. However, it will be shown that this very crude representation of the monopole source term is a fairly good approximation of the acoustic radiation problem.

To make this entire presentation of acoustic source terms meaningful, the theoretical results are compared with data taken in flight on a UH-1H helicopter.¹ In particular, the pressure time history measured on a microphone located nearly in the plane of the rotor tips at a distance of 111 ft is shown in Fig. 6. The nearly symmetrical shape and peak negative amplitude are characteristic of impulsive noise before the onset of radiating shocks.¹⁵ The calculated pressure time history for the simple source and sink at the last 10% of the blade is also shown. Remarkable agreement in pulse shape is apparent although the peak negative pressure is substantially underpredicted. If three sources and sinks are judiciously chosen along the blade chord at the 0.95 radius position, the peak negative amplitude increases slightly and the shape remains

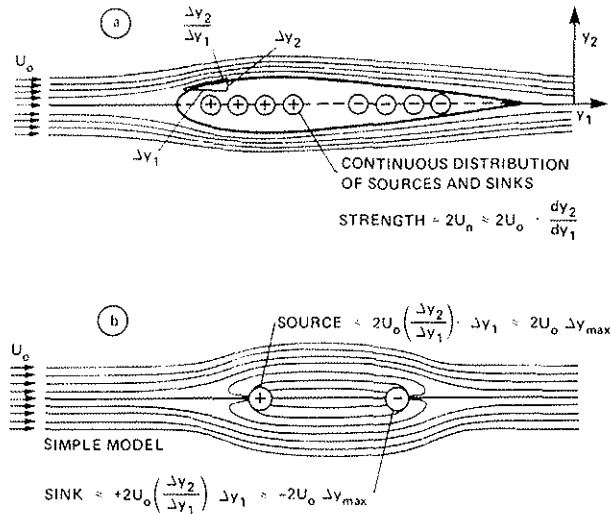


Fig. 5. Monopole source strength.

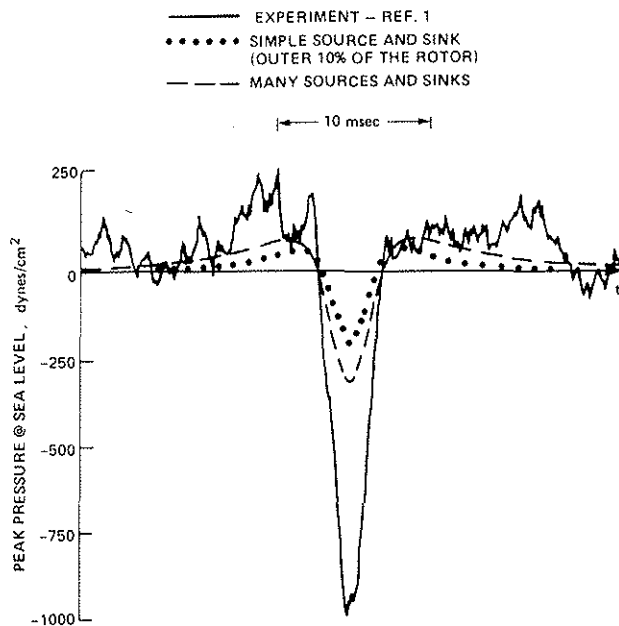


Fig. 6. Monopole thickness noise.

strength while airfoil chord controls first order source and sink positions and thickness distribution controls second order positioning. In practical terms, increases in effective source and sink displacements result in less acoustic cancellation and larger peak pressure amplitudes. Therefore, airfoils with thick leading and trailing edges create more peak negative pressure than those that are thick towards the airfoil center. This simple argument substantiates the detailed calculations of Ref. 12 and provides some physical insight as to why the biconvex airfoil monopole thickness calculations are often lower in peak acoustic amplitude than conventional helicopter airfoils. It also shows that wide chord airfoils will generate more monopole impulsive noise than small chord rotors of the same absolute thickness.

Another important feature of Fig. 6 is that the theory with only monopole thickness underpredicts the radiated noise by a factor of at least 2. Thus, prediction schemes that represent impulsive noise radiation by using monopole thickness noise sources only, may be describing less than half the noise generation process.

Dipole

The second source of radiated noise in Eq. (2) is mathematically represented by the dipole

$$\frac{1}{a_0} \frac{\partial}{\partial t} \int \left[\frac{P_i \cos \theta_i}{r |1 - M_r|} \right] dS(\vec{r})$$

Physically this term represents the time derivative of the amplified sum of local pressure forces exerted by the airfoil on the fluid in the direction of the observer. As is usually done in inviscid two-dimensional airfoil theory, this pressure may be decomposed into that due to thickness and that due to lift.¹⁷ Thus, the pressure on the upper airfoil surface becomes

$$P_u \equiv P_{\text{thickness}} + \frac{\Delta P_{\text{lift}}}{2}$$

and that on the lower surface is

$$P_l \equiv P_{\text{thickness}} - \frac{\Delta P_{\text{lift}}}{2}$$

similar. If a large number of singularities are chosen, the shape continues to remain similar while the amplitude approaches an asymptotic limit which still substantially underpredicts the radiated peak negative pressure. If more radial stations are included, the final calculated shape remains similar and the peak negative pressure from monopole thickness remains underpredicted (Fig. 6).

The interesting feature of Fig. 6 is that the simple source and sink model works so well. Additional sources and sinks do increase the peak negative level somewhat, but do not change the basic shape of the impulsive noise pulse. This implies that general airfoil thickness and chord are really first order effects while thickness distribution for normal airfoil design is a second order parameter. Thickness controls source

where the net lift per unit length along any airfoil section is represented by ΔP . A sketch of both the thickness pressure and the lifting pressure distributions for a symmetrical airfoil section at an angle of attack is shown in Fig. 7. Equal and opposite local pressure forces exerted by the airfoil on the fluid are represented by the small arrows distributed along the airfoil surface.

The contribution to the radiated noise arising from local pressure forces at zero lift is termed the "thickness dipole." As sketched in Fig. 8 for any chordwise station, the components of these fluid pressure forces normal to the mean chord line of the airfoil are equal and opposite and, therefore, produce no radiated noise. (For thin airfoils, surface pressures are assumed to act along the mean chord line.) However, those components that act parallel to the mean chord line add to a nonzero value at each chordwise station. The resulting chordwise distribution of "thickness dipoles" does contribute to the radiated noise (Fig. 8). Computationally, the thickness dipole term is represented by

$$\frac{1}{a_0} \frac{\partial}{\partial t} \sum_{k=1}^{\ell} \sum_{i=1}^n \left[\frac{P_{\text{thickness}} \cos \theta \left(\frac{dy_2}{dy_1} \right)_{ki}}{r |1 - M_r|} \right] dy_{1_i} dy_{3_k} \quad (9)$$

where $\cos \theta = [\vec{r} \cdot (-\vec{e}_{y_1})]/r$ and $-\vec{e}_{y_1}$ is a unit vector along the airfoil chord (forward direction).

As in the case of monopole thickness, the effect of dipole thickness can be modeled quite well by considering a small number of singularities. For the UH-1H example case, six dipoles representing net forces acting parallel to the mean chord line were distributed along each chord at three radial stations comprising the outer 30% of the blade. Local surface pressures were calculated by applying the well-known Prandtl-Glauert compressibility correction to the inviscid incompressible pressure distribution for the two-dimensional NACA 0012 airfoil at zero angle of attack. Calculations for the example case are shown in Fig. 9. The result is a very small amplitude pulse whose shape is quite different from

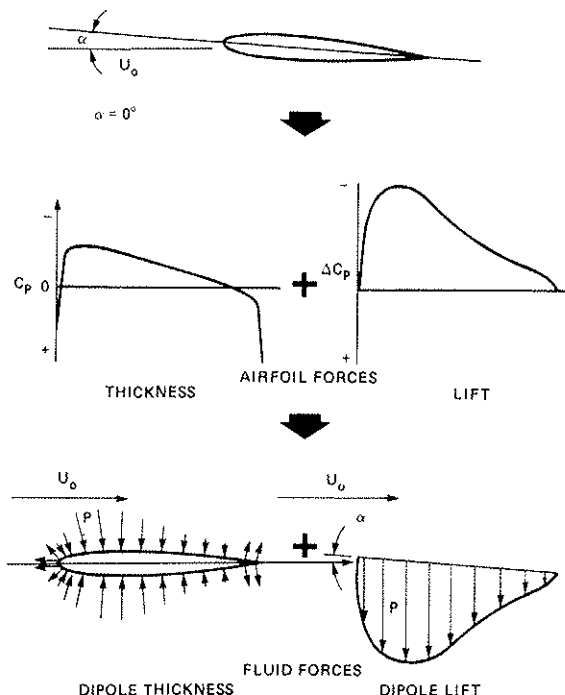


Fig. 7. Separation of thickness and lift airfoil pressure distributions.

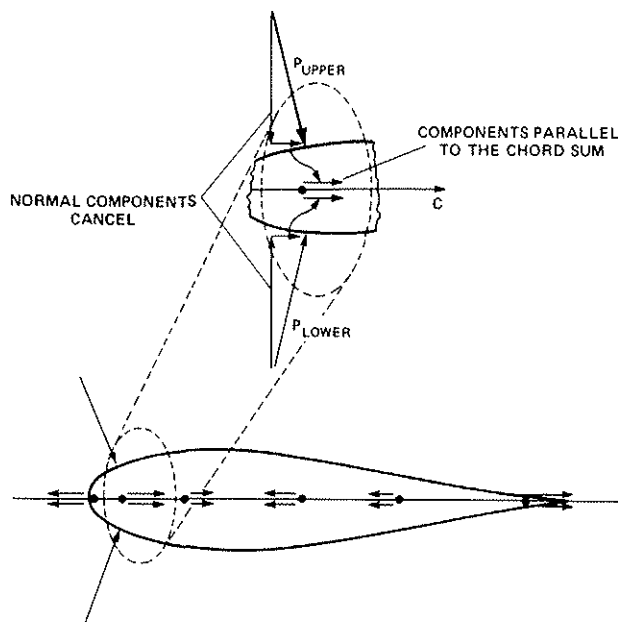


Fig. 8. A simple six-element, two-dimensional model of dipole thickness noise sources.

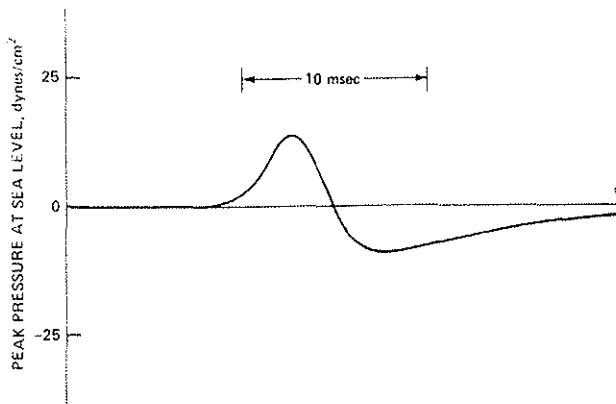


Fig. 9. Dipole thickness noise.

tribution that is expected to be the dominant source of radiated dipole noise because its vector lies nearly within the rotor tip path plane (when $\psi \approx 90^\circ$, $\cos \theta_1 \approx 1$).

Calculations of the drag time history as a rotor blade traverses one revolution and cycles between near stall and transonic conditions are not trivial. Fortunately, it is known from previous investigations¹⁵ that the advancing side of the disc is the major contributor to impulsive noise. In addition, most helicopter designs incorporate blade twist (washout) which shifts the aerodynamic loading at the tip inboard so that the induced drag at $\psi \approx 90^\circ$ is small. In this case, only local transonic effects need be considered. To obtain a realistic estimate of these effects, a finite difference transonic rotor program was run to calculate the peak drag coefficient of the NACA 0012 airfoil at zero lift at the specified conditions. On the basis of this program the peak drag coefficient was assumed constant ($C_D = 0.036$) with azimuthal position and along the rotor span, and the far field radiated dipole drag noise calculated from the expression

$$\frac{1}{a_0} \frac{\partial}{\partial t} \sum_{k=1}^{\ell} \left[\frac{C_D \frac{1}{2} \rho U_0^2 \cos \theta}{r |1 - M_r|} \right] \cdot \text{chord} \cdot dy_{3_k} \quad (10)$$

For simplicity, point dipoles acting at the quarter chord at peak radial stations were assumed. (In this case, distributing the dipole strength along the chord does little to affect the strength or shape of the radiated noise.)

The far field radiated pressure due to this drag dipole model is shown in Fig. 10. The most striking feature of the pressure time history is its asymmetrical shape — it is totally different from that of full scale measurement. It is also apparent that the peak amplitudes are low; this indicates that the effect is quite small on the overall radiated impulsive acoustic signature.

While there are many assumptions in the preceding arguments, it is hard to dispute the fact that aerodynamic forces that act in one direction along the blade and are represented by distributed or concentrated dipoles can be expected to produce a characteristic pressure time history similar to that shown in Fig. 9. Even if the drag force were allowed to first increase from $\psi = 0^\circ$ to $\psi = 90^\circ$, and then decrease from $\psi = 90^\circ$ to $\psi = 180^\circ$ (Ref. 10), there is a net drag on the blade at all times, and this would cause a radiated pressure time history that is basically asymmetric in character and unlike the measured data. Thus, it is difficult to see how these sources of noise could significantly contribute to the measured high-speed impulsive noise phenomena.

Some caution must be exercised in using the above calculations when the microphone is not located near the rotor tip-path-plane. For out-of-plane

measured data. It can be concluded that for typical helicopter conditions, dipole thickness noise is a second order effect.

The remaining part of the dipole contribution to radiated noise is that due to lift for the two-dimensional inviscid airfoil. Fortunately, lift should alter the in-plane acoustic signature little because the lift vector acts normal to the in-plane direction ($\cos \theta_1 \approx 0$). However, in the real environment of the operational helicopter, induced and viscous drag pressure forces must also be considered. In fact, it is the drag con-

locations, local lift effects will become more important ($\cos \theta_1 \neq 0$) and can significantly influence the radiated noise amplitude and temporal shape.

It can be seen from the above calculations and arguments that high speed impulsive noise, as represented by monopole and dipole thickness as well as the second order effect of dipole drag, still underpredicts the measured noise near the plane of the rotor by a factor of about 2. This finding generally agrees with the results of other recent investigations.

Quadrupole

The last and most subtle contribution to high-speed impulsive noise is traceable to the quadrupole term in Eq. (2)

$$\frac{1}{a_0^2} \frac{\partial}{\partial t} \int \left[\frac{\cos \theta_1 \cos \theta_j}{r |1 - M_r|} \frac{\partial T_{ij}}{\partial t} \right] dV(\vec{y})$$

where

$$T_{ij} = \rho u_i u_j + P_{ij} - a^2 \rho \delta_{ij}$$

It can be argued that the $(P_{ij} - a^2 \rho \delta_{ij})$ term, which is due to viscous stresses, variable sound speed, and heat conduction, is probably small for most helicopter rotors operating near or less than an advancing tip Mach number of 1. However, the $\rho u_i u_j$ term is not so easily dismissed. In fact, it will be shown to be the most important part of high-speed impulsive noise. Substituting $T_{ij} \approx \rho u_i u_j$ into the quadrupole term yields

$$\frac{1}{a_0^2} \frac{\partial}{\partial t} \int \left[\frac{\cos \theta_1 \cos \theta_j}{r |1 - M_r|} \frac{\partial (\rho u_i u_j)}{\partial t} \right] dV(\vec{y}) \quad (11)$$

In general there are nine separate components to the $\rho u_i u_j$ term.

This implies that it is necessary to know enough of the details of the unsteady and possibly transonic flow field surrounding the blade to be able to evaluate each term. While this is true, especially for unsteady transonic flow, the situation is not all that hopeless. The far-field radiated noise is most sensitive to the gross features of the local flow field at subsonic Mach numbers. Thus, those components of $\rho u_i u_j$, which mathematically represent the largest variations in the distributed flow field over the nearby volume of fluid surrounding the blade, are the most likely contributors to the radiated noise. Using this reasoning, and expanding $\rho u_i u_j$ into its effective components in two dimensions,

$$\begin{aligned} \rho u_i u_j &= \rho(U_0 + \Delta u_1)(U_0 + \Delta u_1) + \rho(U_0 + \Delta u_1)\Delta u_2 \\ &+ \rho(\Delta u_2)(U_0 + \Delta u_1) + \rho(\Delta u_2)^2 \end{aligned} \quad (12)$$

For simplicity in this calculation, consider the symmetrical NACA 0012 airfoil and assume it is operating at zero lift. In this simple nearly in-plane radiation case, it can be argued that variations in Δu_2 over the upper and lower surfaces of the airfoil will cancel leaving

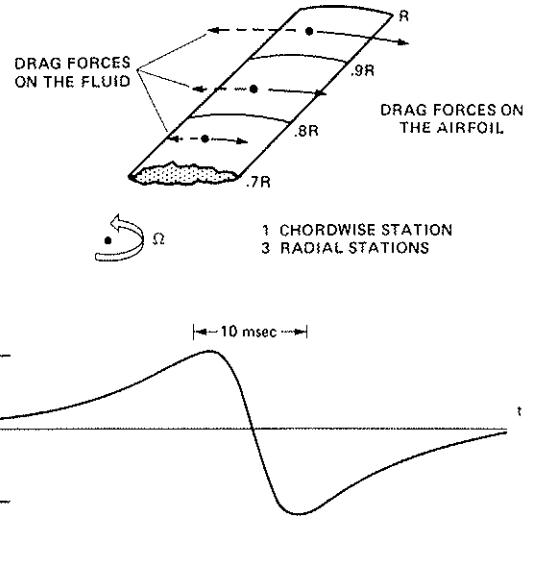


Fig. 10. Dipole drag noise.

$$\rho u_i u_j \approx \rho(U_0 + \Delta u_1)(U_0 + \Delta u_1) \quad (13)$$

It can also be argued that variations in U_0 are really quite small over the same interval when compared to changes in Δu_1 ; therefore

$$\rho u_i u_j \approx 2\rho U_0 \Delta u_1 + \rho \Delta u_1^2 \quad (14)$$

Neglecting second order terms in Δu_1 and substituting this expression into (11) yields

$$\frac{1}{a_0^2} \frac{\partial}{\partial t} \int \left[\frac{2\rho \cos^2 \theta}{r|1 - M_r|} U_0 \frac{d(\Delta u_1)}{dt} \right] dV(\vec{y}) \quad (15)$$

$$\cos \theta_i = \cos \theta_j = \cos \theta$$

For first calculation purposes, it is further assumed that steady incompressible airfoil theory can be used to calculate the flow field surrounding the NACA 0012 airfoil at zero angle of attack. A sketch of the variation over the airfoil is given in Fig. 11 for three chordwise stations. Fortunately, the Δu_1 component is negligible at distances greater than three chord lengths from the airfoil. At any position along the airfoil in steady flow,

$$\frac{d(\Delta u_1)}{dt} = \frac{d(\Delta u_1)}{dy_1} U_0$$

Therefore, (15) can be rewritten as

$$\frac{1}{a_0^2} \frac{\partial}{\partial t} \int \left[\frac{2\rho \cos^2 \theta}{r|1 - M_r|} U_0^2 \frac{d(\Delta u_1)}{dy_1} \right] dV(\vec{y}) \quad (16)$$

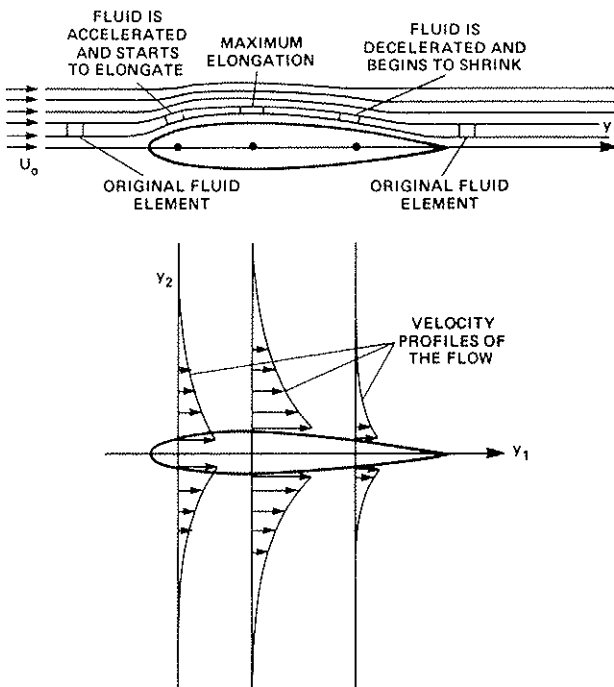


Fig. 11. Flow field of a two-dimensional airfoil.

Equation (16) does have a simple physical explanation. Consider the two-dimensional airfoil sketched in Fig. 11. As a fluid element passes over the airfoil, it is first accelerated and elongated and then decelerated and compressed returning to its original size in the freestream behind the airfoil. Consider an elemental volume fixed to the airfoil coordinate system. To first order in Δu_1 , the Eulerian momentum equation for steady flow in the y_1 direction is

$$-\frac{\partial P_1}{\partial y_1} = 2\rho U_0 \frac{\partial(\Delta u_1)}{\partial y_1} \quad (17)$$

which appears as a factor in Eq. (16). Physically, the pressure gradient in the chordwise direction is balancing the inertial force of the fluid. There is no net force on the fluid and thus no dipole radiation. However, because momentum flux changes in the chordwise direction create a pressure gradient, a longitudinal quadrupole source results which can radiate

acoustic energy. The numerical form of Eq. (16) becomes

$$\frac{1}{a_0^2} \frac{\partial}{\partial t} \sum_{k=1}^{\ell} \sum_{i=1}^n \sum_{j=1}^m \left[\frac{2\rho \cos^2 \theta}{r|1 - M_r|} U_0^2 \frac{d(\Delta u_1)}{dy_{1_i}} \right] dy_{2_j} dy_{1_i} dy_{3_k} \quad (18)$$

Although in principle the quadrupole expression requires the retarded time integration over the volume exterior to the airfoil, the calculation is simplified by symmetry. All of the resulting longitudinal quadrupoles are symmetrical about the chord line of the airfoil. For a nearly in-plane microphone position, all longitudinal quadrupoles on any line perpendicular to the chord line of the airfoil can be summed at the same retarded time. Therefore, the velocity variation along y_2 can be summed to form a total integrated velocity change.

$$A_u = \sum_{j=1}^m \Delta u_1 dy_{2j} \quad (19)$$

where A_u is a function of y_1 and y_3 and has the dimensions of ft^2/sec . Figure 12 illustrates how $A_u/(U_o \cdot c)$ varies versus airfoil chord for the NACA 0012 airfoil in steady subsonic compressible flow. Using this definition, the numerical form of Eq. (18) becomes

$$2\rho \left(\frac{U_o}{a_o}\right)^2 \frac{\partial}{\partial t} \sum_{k=1}^{\ell} \sum_{i=1}^n \left[\frac{\cos^2 \theta}{r|1 - M_r|} \frac{d(A_{u_{ki}})}{dy_{1i}} \right] dy_{1i} dy_{3k} \quad (20)$$

The total effect of the quadrupole field has been replaced by a distribution of singularities $d(A_{u_{ki}})/dy_{1i}$ along the mean line of the rotor blade. These simple singularities are treated in exactly the same manner as the monopole and dipole contributions to the impulsive noise. The acoustic field in the simplest case — that is, with an effective point quadrupole pointing forward over the front part of the airfoil and another point quadrupole pointing rearward for the last 10% of the blade — is shown in Fig. 13 for the UH-1H helicopter flying at 80-knots IAS. The shape closely matches the measured data and the contribution to radiated impulsive noise is significant. For a large number of singularities distributed over the blade chord and span, the shape remains similar and the amplitude grows to about one-half the peak pressure level measured in flight. It may be concluded, based on these simple physical arguments, that quadrupole radiation is an important part of high-speed noise.

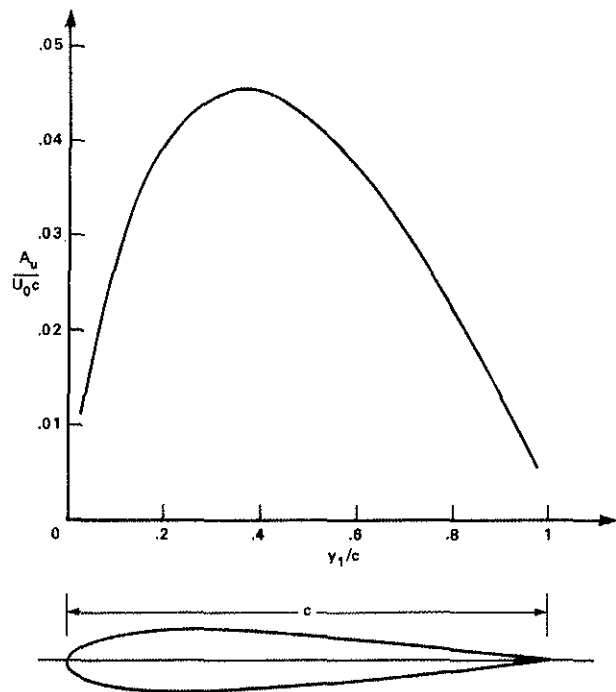


Fig. 12. Nondimensional integrated velocity disturbance ($A_u/U_o c$) as a function of chord.

A final plot comparing the monopole plus dipole model and the monopole plus dipole plus quadrupole model with experiment is shown in Fig. 14 for the 80-knot data point. As indicated previously, the theoretical model which incorporates only monopole and dipole sources underpredicts the far field in-plane radiated noise by at least a factor of 2. However, when quadrupole thickness sources are added to the monopole and dipole sources, the prediction of the measured noise signature closely matches both the shape and amplitude of the measured data.

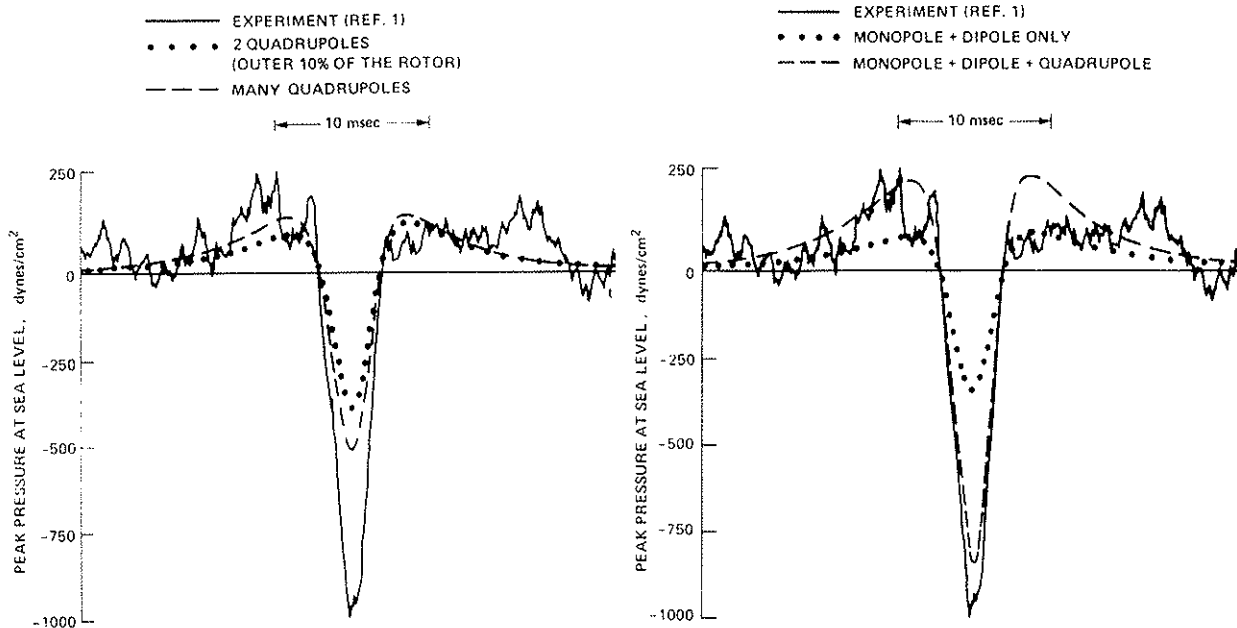


Fig. 13. Quadrupole thickness noise.

Fig. 14. Monopole plus dipole and monopole plus dipole plus quadrupole contributions to radiated impulsive noise.

5. Further Comparison With Experiment

It has been quite natural in the previous sections of this paper to trace the aerodynamic origins of impulsive noise by using the pressure time history of the radiated noise. Peak amplitudes and impulse shapes of theory versus experiment were easily compared. For deterministic impulsive noise, it is important to realize that these time domain analyses are much better (more quantitative) measures of impulsive noise than power spectra of the same event. As shown, a careful time domain analysis of the radiated noise isolates the basic aerodynamic cause. Therefore, the following comparisons of theory and experiment continue to rely on time domain characteristics of the impulsive noise signal; in particular, peak negative amplitudes and temporal shapes are compared.

Figures 15 and 16, taken from Ref. 1, illustrate the lateral and longitudinal directivity of impulsive noise for the 80- and 115-knot IAS cases of the UH-1H helicopter. The peak amplitudes shown in these figures should only be treated qualitatively because of relatively large excursions in separation distance between the rotor and the microphone during the testing. Also shown on these plots are the peak levels predicted by the present theoretical model incorporating monopole, dipole, and quadrupole thickness noise sources. At 80-knots IAS (Fig. 15), comparison with experiment is quite good in amplitude for all lateral and longitudinal microphone positions. At 115-knots IAS (Fig. 16), theory and experiment are reasonably close but do not compare as favorably as in the 80-knot case. However, comparison of the current theoretical model with the monopole-dipole model of Hawkins and Lawson¹⁴ shows the current model to more nearly represent the phenomena of high-speed impulsive noise. As noted in the introduction, none of the analyses to date has included quadrupole contributions to the radiated noise and, therefore, all have under-predicted its level.

A more definitive comparison of the present theory with experiment is shown in Fig. 17. Advancing tip Mach number of the helicopter's main rotor is known to be a primary parameter in the generation of impulsive noise.¹⁵ Therefore, peak pressures measured on a microphone located nearly within the tip-path-plane

of the rotor directly in front of the helicopter are plotted in Fig. 17; the peak pressures are plotted versus advancing tip Mach number. The data were gathered from two separate in-flight test programs; the first utilizing a OV-1C aircraft¹ and the second utilizing a YO-3A "quiet" aircraft as the measurement platform. A nominal separation distance of 75 ft between the aircraft and the subject helicopter was attempted. As indicated in Ref. 1, this distance was not maintained consistently during acoustic testing with the OV-1C. Therefore, the peak pressures from this test, which are shown in Fig. 17, have been corrected in level to the desired 75-ft separation distance by using the standard $1/r$ pressure amplitude change with separation distance. In the second flight test program, the nominal separation distance was held much more accurately (± 5 ft). Therefore, the data from this test, which are shown in Fig. 17, have not been scaled with separation distance.

The data from both in-flight tests establish a consistent trend. As previously noted by many investigators, peak pressure levels of impulsive noise increase dramatically with increases in advancing tip Mach number. The peak pressure levels, which are calculated by utilizing the present theoretical model, are also shown in Fig. 17. At low advancing tip Mach numbers ($M_{AT} \approx 0.8 \rightarrow 0.87$), good agreement with data is apparent. As the advancing tip Mach number increases, the calculated and peak pressure amplitudes show only fair agreement.

The strengths and limitations of the theoretical model can be illustrated further by comparing the calculated and measured pressure time histories (bottom of Fig. 17). At moderate tip Mach numbers, theory and experiment compare quite well in both amplitude and shape as explained in the previous section of this paper.

However, as shown in the bottom right of Fig. 17, theory and data do not compare as favorably at higher advancing tip Mach numbers. The theoretical predictions are basically symmetrical pulses and the measured data are sawtooth pulses of larger amplitude and width. The sharp pressure rise of the high advancing tip Mach number measured pulse is indicative of a radiating shock wave.¹⁵ The fact that the current model cannot predict this event is not too surprising; the assumed aerodynamic model and the neglect of the $P_{ij} - a^2 \rho \delta_{ij}$ term in the

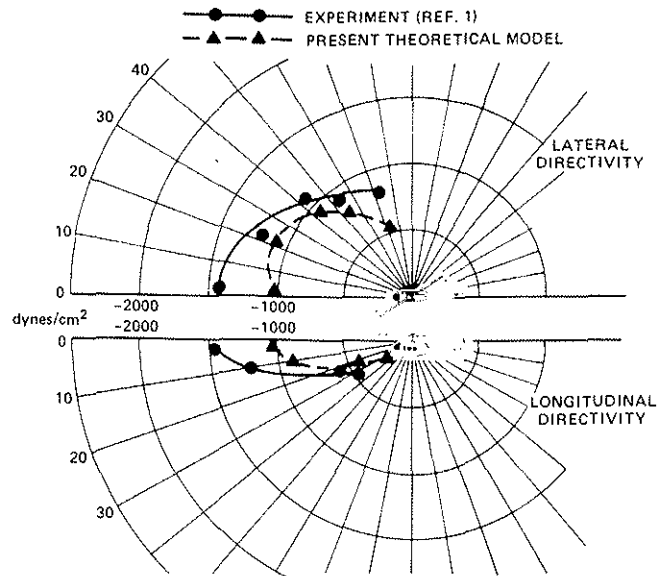


Fig. 15. Directivity of peak negative pressure pulse (80-knots IAS and 400 ft/min R/D).

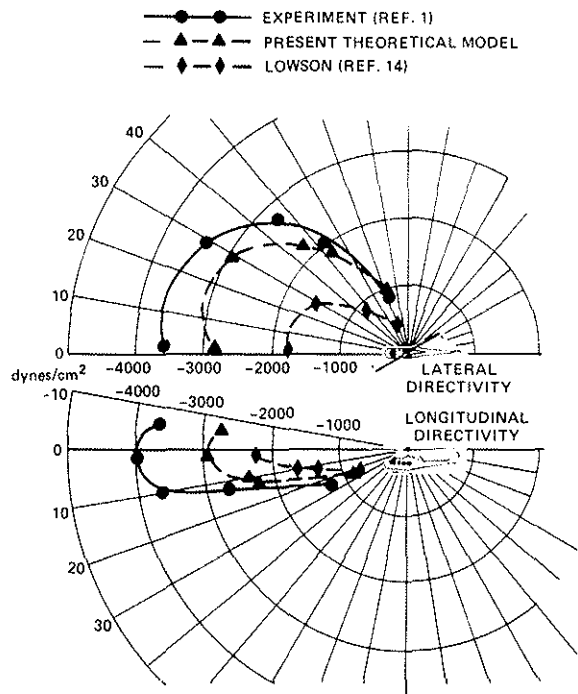


Fig. 16. Directivity of peak negative pressure pulse (115-knots IAS, level flight).

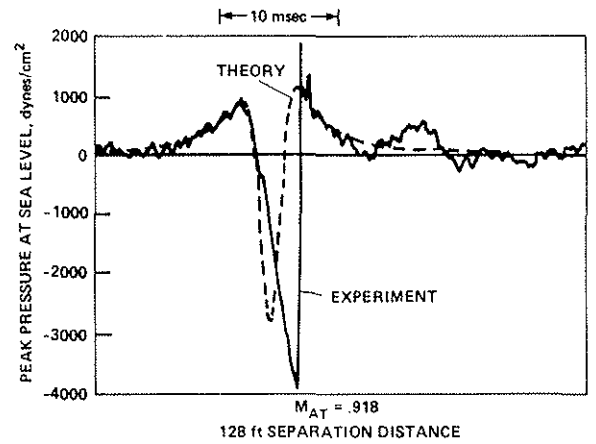
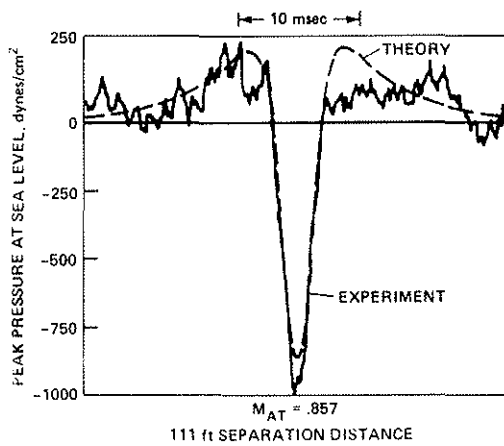
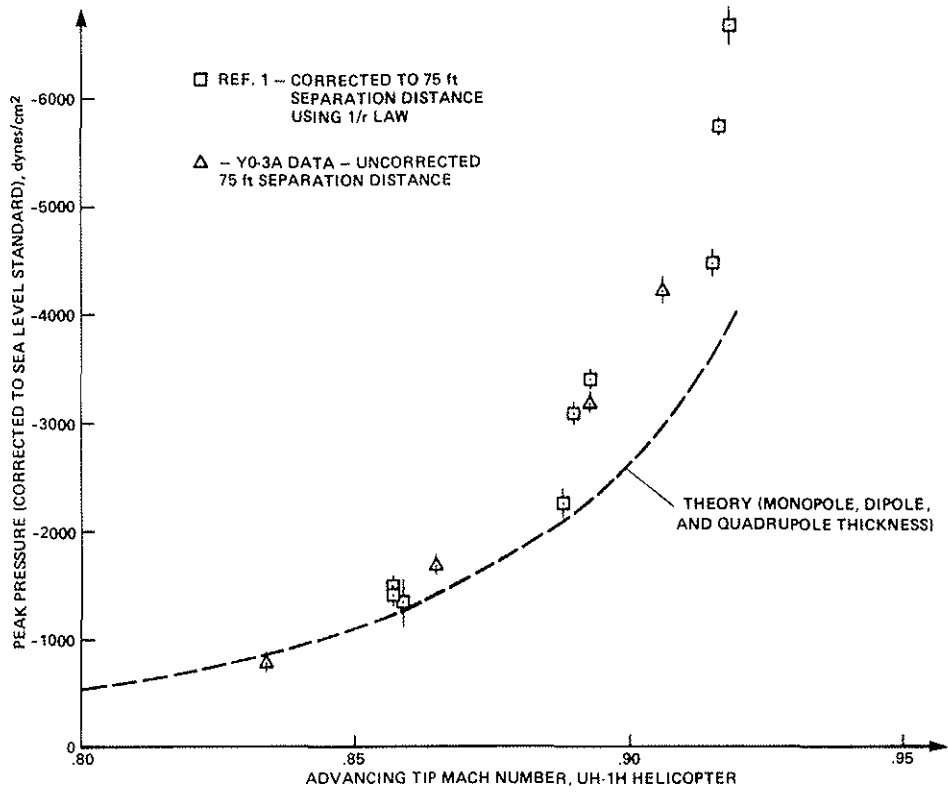


Fig. 17. Theory versus experiment as a function of advancing tip Mach number.

acoustic formulation of this simple approach, do not incorporate any transonic or unsteady phenomena. The apparent success of this simple model below an advancing tip Mach number of 0.9 for an NACA 0012 airfoil, indicates that these nonlinear and unsteady aerodynamic phenomena become important for the calculation of impulsive noise when they occur over a substantial portion of the rotor disc. Fortunately, the next generation of helicopters in the United States employ thinner airfoil sections and operate at lower advancing tip Mach numbers. Therefore, the impulsive radiating shock signature of the UH-1H (bottom right of Fig. 17) is not a characteristic of these newer vehicles. For these new helicopters, the current theoretical model, which incorporates quadrupole thickness noise sources in addition to monopole and dipole noise sources, should work quite well.

6. Some Additional Thoughts

The finding that the volume of fluid surrounding the high-speed rotor (or propeller) is important in the generation of in-plane impulsive noise naturally leads to the question: How important is quadrupole noise over the entire Mach number range? Of course, extreme care must be exercised when answering this question. The model itself is marginal above an effective Mach number of 0.9 for reasons already mentioned. At much lower advancing tip Mach numbers, the severity of the noise decreases dramatically — so much so, that thickness noise may not be the dominant noise source. Nevertheless, it is instructive to estimate the magnitude of the competing in-plane noise sources.

As shown in Fig. 18, in-plane thickness noise for the NACA 0012 airfoil at a constant advance ratio dramatically decreases in amplitude with reductions in advancing tip Mach number. (Note the log scale for peak pressure amplitude.) It is also significant to observe that quadrupole thickness is the largest contributor to the radiated acoustic field above an advancing tip Mach number of approximately 0.5. Near Mach number 0.9, quadrupole thickness sources account for about 60% of the radiated in-plane noise. Below an advancing tip Mach number of 0.5, monopole thickness becomes the larger contributor to the very weak acoustic field.

In principle, a more accurate estimate of in-plane impulsive noise for 12% and thicker airfoils operating above an advancing tip Mach number of 0.9 is quite straightforward. However, much care must be observed in both the solution and modeling of acoustic sources and the modeling of aerodynamic boundary conditions. With shocks and a local supersonic region present over a significant portion of the rotor disc, the assumptions of no heat conduction, constant speed of sound, and negligible viscous stresses should be questioned. The change to the acoustic equations is that the stress tensor, T_{ij} , should include the terms, $P_{ij} - a^2\rho\delta_{ij}$. In addition, there are several

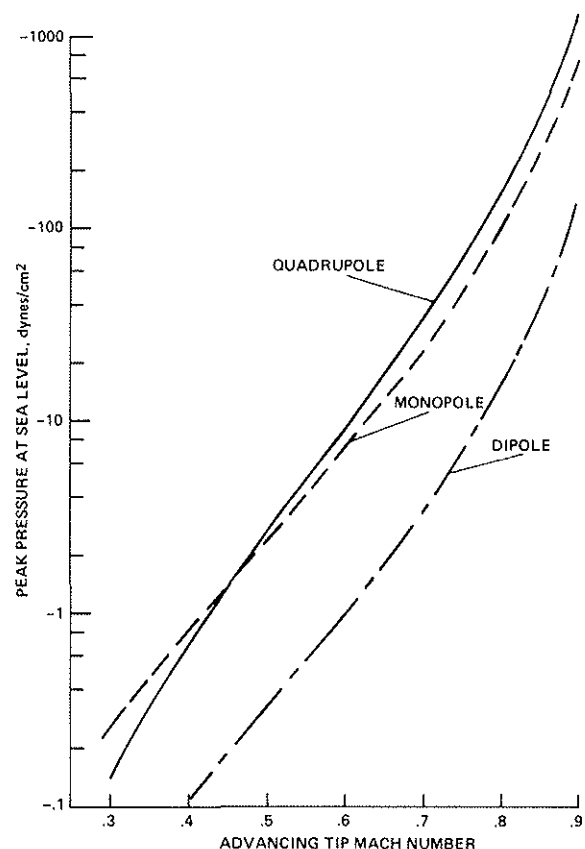


Fig. 18. Relative contribution of sources to in-plane acoustic radiation.

aerodynamic questions that should be addressed — all of which could be significant in the accurate prediction of the pressure time history.

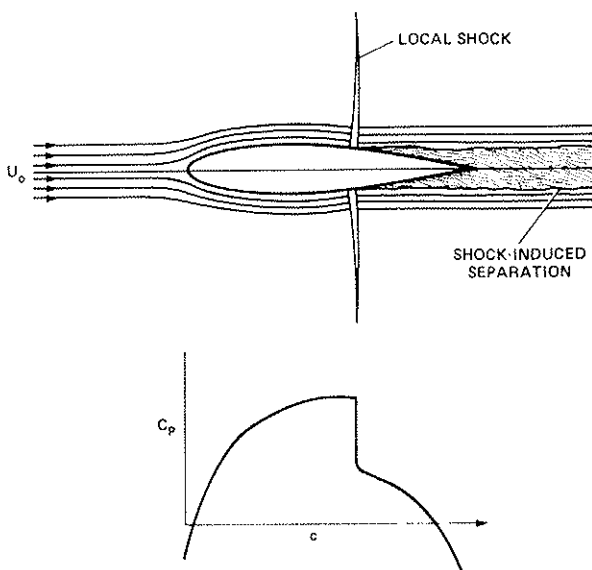


Fig. 19. A sketch of the aerodynamic environment of the transonic rotor.

Consider the two dimensional sketch (Fig. 19) of a section of a helicopter rotor at transonic Mach numbers. Local transonic aerodynamic effects become important and alter the entire flow field. The point of minimum pressure shifts rearward, leading to the formation of a local attached shock. This usually causes separation over the trailing edge of the airfoil. For the rotor, this picture is further complicated by the fact that the flow field is unsteady and three dimensional (especially near the tip). Aerodynamically, such problems are solved in the near field using numerical techniques.¹⁸ Using these solutions, in principle, it is possible to specify the correct monopole, dipole, and quadrupole sources necessary to accurately describe the acoustic far field.

The current theory does shed some light on the most important practical question: How can the helicopter designer reduce high-speed impulsive noise? Fortunately, some of the more obvious solutions have already been arrived at through trial and error and the requirement that high-speed aerodynamic loads be kept to a minimum. First, the advancing tip Mach number and, therefore, the hover tip Mach number, should be kept as low as possible; this is the most efficient method of reducing the amplification of in-plane acoustic energy. Its main disadvantage as a design rule is that the helicopter will weigh more (thus be more expensive) for the same mission compared with a helicopter utilizing a high tip speed rotor. Secondly, the tip of the rotor blades should be thinned as much as possible — remembering that the most acoustically efficient place on the rotor is at the tip but that the rotor also has to operate in a region near maximum lift on the retreating side of the disc. On current helicopters, this rule has evolved to a thickness ratio of from 6 to 9% in the tip region.

A more subtle result of the current simple model is the idea that "sweeping" the tip of the rotor will reduce high-speed impulsive noise. By sweeping the blade, the phase of the simple sources can be positioned to facilitate cancellation in the far field. This, too, has been tried with some success in the industry. However, the current theory suggests that there are definitely more optimum methods of combining the important parameters to achieve less noise than those previously tried.

7. Concluding Remarks

Perhaps the most important finding of this present study is that the phenomenon of high-speed impulsive noise is a manifestation of large scale aerodynamic effects. The smaller details of the local flow and pressure fields surrounding the rotor blade are not necessary for the prediction of far field radiated noise when local compressibility effects are not severe. However, it has been shown that the resulting simple acoustic model must incorporate monopole, dipole, and quadrupole noise sources. Correct estimation of the strength of these sources requires knowledge of the entire flow field surrounding the rotor — not just an estimate of local thickness and pressure distributions.

The neglect of quadrupoles as noise sources by previous investigators has sometimes been rationalized by classical arguments — comparing a single stationary quadrupole's radiation efficiency with the dipole and monopole. Although the single stationary quadrupole is admittedly less efficient, the flow field surrounding the rotor includes an effective volume of moving quadrupole sources which, when added together, become important in the far acoustic field of the helicopter.

The establishment of quadrupoles as noise sources for helicopters may have important implications for the prediction and control of all rotor equipment. As in the case of the helicopter, it may well be that the peak pressure level, especially at in-plane positions, has been characteristically underpredicted because of the neglect of these important noise sources.

ACKNOWLEDGMENTS

The authors are indebted to many people at the Ames Directorate of the U.S. Army Air Mobility R&D Laboratory for their unselfish contributions. In particular, our colleague, Mr. Donald Boxwell, helped with both conceptual and experimental inputs, and Mr. Rande Vause was responsible for our initial computational algorithm. Several transonic calculations were provided by Mr. Frank Caradonna. We also thank Mr. H. Andrew Morse for his consistent and untiring support.

REFERENCES

1. F. H. Schmitz and D. A. Boxwell, In-flight far field measurement of helicopter impulsive noise, J. of American Helicopter Society, Oct. 1976.
2. L. Gutin, On the sound field of a rotating propeller, Phys. Z. Sowjetunion, 9, 57, 1936. Trans. NACA TM-1195, 1948.
3. I. E. Garrick and C. E. Watkins, A theoretical study of the effect of forward speed on the free-space sound pressure field around propellers, NACA Rep. No. 1198, 1954.
4. A. F. Deming, Noise from propellers with symmetrical sections at zero blade angle, NACA TN No. 679, 1938.
5. M. J. Lighthill, On sound generated aerodynamically, I. General Theory, Proceedings of the Royal Society, Series A, Vol. 211, 1952, pp. 564-587.
6. N. Curle, The influence of solid boundaries upon aerodynamic sound, Proceedings of the Royal Society, Series A, Vol. 231, 1955, pp. 505-514.
7. M. V. Lowson, A theoretical study of helicopter rotor noise, J. Sound and Vibrations, Vol. 9, 1967, pp. 197-222.
8. S. E. Wright, Sound radiation from a lifting rotor generated by asymmetric disk loading, J. Sound and Vibration, Vol. 9, No. 2, 1969, pp. 223-240.
9. R. H. Lyon, Radiation of sound by airfoils that accelerate near the speed of sound, J. Acoustical Society American, 49, 1971, pp. 894-905.
10. R. E. Arndt and D. C. Borgman, Noise radiation from helicopter rotors operating at high tip Mach numbers, J. American Helicopter Society, 16, 36-45, 1971.
11. J. E. Ffowcs Williams and D. L. Hawkings, Sound generation by turbulence and surfaces in arbitrary motion, Philosophical Transactions of the Royal Society of London, Series A, Vol. 264, May 8, 1969, pp. 321-342.
12. F. Farassat, Theory of noise generation from moving bodies with an application to helicopter rotors, NASA TR R-451, Dec. 1975.
13. D. L. Hawkings and M. V. Lowson, Theory of open supersonic rotor noise, J. Sound and Vibration, Vol. 36, No. 1, 1974, pp. 1-20.

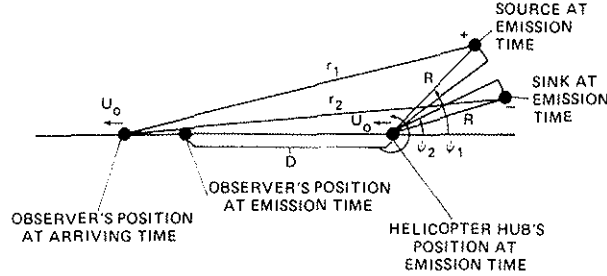
14. M. V. Lowson, Research requirements for the improvements of helicopter operations, AGARD Rotorcraft Design Symposium, Ames Research Center, May 1977.
15. C. R. Vause, F. H. Schmitz, and D. A. Boxwell, High-speed helicopter impulsive noise, Presented at the 32nd Annual National V/STOL Forum of the American Helicopter Society, Washington, D.C., May 1976.
16. J. E. Ffowcs Williams and D. L. Hawkings, Theory relating to the noise of rotating machinery, J. Sound and Vibration, Vol. 10, No. 1, 1969, pp. 10-21.
17. I. H. Abbott and A. E. Von Doenhoff, Theory of Wing Sections, Dover Publications, Inc., 1949.
18. F. X. Caradonna and M. P. Isom, Numerical calculation of unsteady transonic potential flow over helicopter rotor blades, AIAA Journal, Vol. 14, No. 4, April 1976, pp. 482-488.

APPENDIX

In order for signals from two separate positions on the rotor blade to reach the observer simultaneously, the following equation should be satisfied

$$\frac{r_1}{a_o} + \frac{\psi_1}{\Omega} = \frac{r_2}{a_o} + \frac{\psi_2}{\Omega} \quad (A1)$$

where notations are defined in the following sketch of the retarded time geometry.



From simple geometry, the following expression for r_i and ψ_i is obtained.

$$\left[1 - \left(\frac{U_o}{a_o} \right)^2 \right] r_i^2 = 2 \frac{U_o}{a_o} (D + R_i \cos \psi_i^*) r_i - (D^2 + 2DR_i \cos \psi_i^* + R_i^2) = 0 \quad (A2)$$

where

$$\psi_i^* = \begin{cases} \psi_1 & \text{for } i = 1 \\ \psi_2 - \text{azimuthal angle between source positions (radians)} & \text{for } i = 2 \end{cases}$$

For a given azimuthal position of the first source, that is ψ_1 , the position of the second, ψ_2 , can be found by minimizing the function F using standard techniques.

$$F = - \frac{\Omega}{a_o} (r_1 - r_2) + \psi_2 - \psi_1 \quad (A3)$$

Additional source positions are found by repeated application.